



International Conference on Concentrating Solar Power and Chemical Energy Systems,
SolarPACES 2014

Advanced multiphysics modeling of solar tower receivers using object-oriented software and high performance computing platforms

G. Colomer^a, J. Chiva^b, O. Lehmkuhl^{a,b}, A. Oliva^{b*}

^aTerma Fluids SL, Av. Jacquard 97 1-E, 08222 Terrassa, Barcelona, Spain

^bCentre Tecnològic de Transferència de Calor (CTTC), Universitat Politècnica de Catalunya (UPC), ETSEIAT, Colom 11, 08222 Terrassa, Barcelona, Spain

Abstract

This paper presents an advanced methodology for the detailed modeling of the heat transfer and fluid dynamics phenomena in solar tower receivers. It has been carried out in the framework of a more ambitious enterprise which aims at modeling all the complex heat transfer and fluid dynamics phenomena present in central solar receivers. The global model is composed of 4 sub-models (heat conduction, two-phase flow, solar and thermal radiation and natural convection) which are described. Results of the numerical model obtained so far are also presented and discussed

© 2015 Published by Elsevier Ltd. This is an open access article under the CC BY-NC-ND license (<http://creativecommons.org/licenses/by-nc-nd/4.0/>).

Peer review by the scientific conference committee of SolarPACES 2014 under responsibility of PSE AG

Keywords: numerical model; solar tower; CFD&HT

1. Introduction

Solar thermal energy is becoming a very important renewable energy, with large scale plants operating in different parts of the world [1]. There are different designs for solar power collectors that are currently being used to generate electricity, like parabolic trough, parabolic dish and solar tower. In a solar tower plant, the solar radiation is reflected and concentrated by a field of mirrors into a receiver. Panels of tubes with circulating water receive this

* Corresponding author. Tel.: +34-937-398-192;
E-mail address: cttc@cttc.upc.edu

radiation and steam is produced. This steam is used to power turbines in order to generate electrical energy. The heat transfer and fluid dynamics phenomena in the receiver are the interest of this study. The purpose of the current work is to describe the numerical model of a saturated steam solar receiver, which includes sub-models for heat conduction, two-phase flow, solar and thermal radiation and turbulent natural convection.

TermoFluids [2], a general purpose unstructured and parallel object-oriented computational fluid dynamics (CFD) code developed to solve industrial flows, is used in this work.

2. Definition of the modeling

A scheme of a solar tower field is given in Fig. 1a. The receiver is composed essentially by an array of tubes but different designs for the tubes and the structure of the receiver are considered in the model (tubes with fins, different angles, grouped in panels, inside a cavity, cylindrical, with or without back-insulation, more than one level of arrays, etc.). Two possible configurations are shown in Fig. 1b (horizontal finned tubes inside a cavity with back-insulation) and Fig. 1c (portion of a cylindrical receiver with vertical tubes and back-insulation).

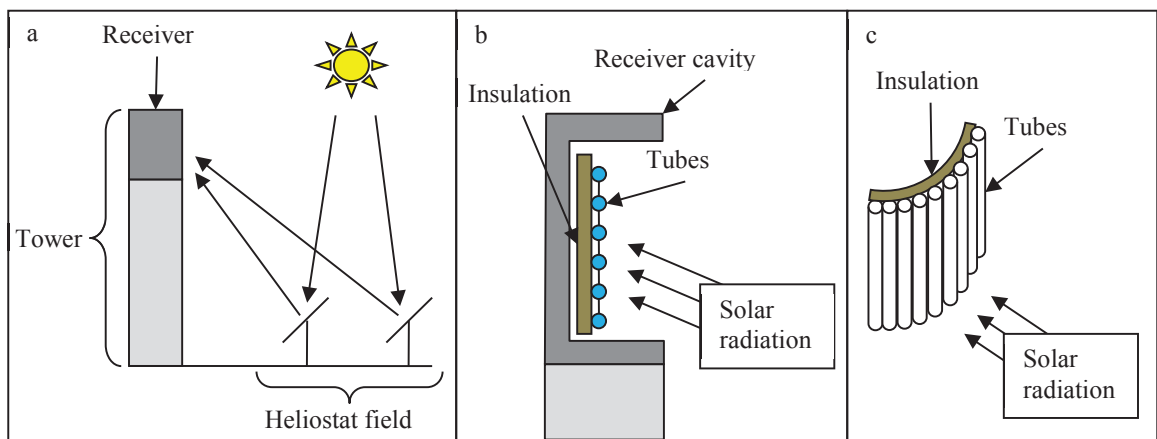


Fig. 1. (a) Scheme of a solar tower power plant; (b) Scheme of receiver cavity; (c) Scheme of a portion of a cylindrical receiver.

The mathematical model considers:

- Transient conduction heat transfer at the solid elements of the receiver (tubes shown in Fig. 1b and Fig. 1c).
- Two-phase flow inside the tubes of the receiver.
- Solar radiation received by the tubes.
- Radiative heat transfer between the surfaces of the receiver.
- Convective heat transfer between the tubes and the air surrounding them.

2.1. Heat conduction in the solid elements of the solar receiver

Transient conduction heat transfer can be solved directly from the governing equation. For the case of transient heat conduction without volumetric sources, the energy transport equation can be written in integral form as:

$$\rho c_p \frac{\partial T}{\partial t} = \nabla \cdot (\lambda \nabla T) \quad (1)$$

where T represents temperature, t is the time, ρ is density, c_p is the specific heat and λ the thermal conductivity. Unfortunately, due to the geometry of the receivers considered by the model presented, a correct evaluation of conduction heat transfer is not straightforward. The width of the tubes is of the order of millimetres while the overall

receiver is of the order of meters. In order to solve eq. 1 using finite volume techniques, large meshes have to be used to solve the heat transfer at the tubes, and parallel computers are needed. In this work, a non-structured mesh has been used, so that extensions to other geometries of the tubes can be implemented without substantial changes. A parametric mesh generator has been designed and implemented in order to reduce the time needed to change the density of the mesh or the number of tubes. This program allows to obtain meshes with different densities and number of tubes and also to concentrate the control volumes at the critical points (for example, the union between tubes and fins of a receiver with that configuration).

In TermoFluids, for the integration of the governing equations the finite control volume method has been used. A modified least-square method has been chosen for the calculation of the gradients. The resulting system of equations is solved by means of the Conjugate Gradient method [2].

The conduction model links all the other models through boundary conditions:

- Insulation at the back side of the tubes: The back side of the tubes of the receiver may be covered with an insulating material. This situation is simulated using a one dimensional approach to obtain the value of the heat flux between the tubes and the air in contact with the insulating material:

$$q = \alpha \lambda \left(\frac{T_w - T_g}{\lambda + \alpha \Delta x} \right) \quad (2)$$

where q is the heat flux, α is the convective heat transfer coefficient, λ is the thermal conductivity of the insulator material, T_w and T_g are the temperature of the external wall of the tube and the temperature of the air respectively and Δx is the thickness of the insulator.

- Solar radiation at the tubes of the receiver: The radiation reflected by the heliostats to the receiver is distributed on the tubes. This distribution depends on the particular arrangement and the absorptivity of the tubes, and the incidence direction of the solar radiation. This input can be given to the convection-conduction simulation code.
- Thermal radiation at the surfaces of the receiver: the radiative heat transfer between the surfaces of the receiver can be calculated using the radiosity method, or using a Monte Carlo Ray Tracing (MCRT) tool. Using the former, more efficient method, the view factors are calculated by taking multiple reflections into account, and including the fact that any given tube will see only a part of some other tubes. A calculation using only the MCRT tool is possible, although significantly more expensive in terms of computational cost.
- The convective heat transfer between the tubes and the air of the cavity is calculated using the Newton's law of cooling:

$$q = \alpha(T_w - T_g) \quad (3)$$

and the convective heat transfer coefficient α is calculated from the Nusselt number (obtained as described in section 2.4):

$$\alpha = \frac{\lambda Nu}{L} \quad (4)$$

where λ is the thermal conductivity of the air and L is the characteristic length.

- Forced convection inside the tubes: The convective heat transfer between the internal flow of the fluid and the tubes of the panels is calculated using Newton's law of cooling. The temperature of the fluid and the convective heat transfer coefficient are obtained from the two-phase flow model described in next section.

2.2. Two-phase fluid flow inside the tubes

The evaporation phenomena inside the tubes cannot be solved directly from the governing equations (mass, energy and momentum conservation), because instantaneous tracking of the vapor-liquid inter-phase is too complex to do so.

In this work, a one dimensional quasi-homogeneous model has been chosen to represent the forced convection in the tubes, solved by the step by step method, which was used in the numerical analysis of two-phase flow inside tubes [3]. The fact that this code is one dimensional makes difficult the communication between the two-phase flow code and the code for the solid elements. This problem has been solved calculating one heat transfer coefficient and one average wall temperature obtained from evaluating the energy conservation equation at the walls of the pipes.

For this model, the crux of the matter is the critical heat flux (CHF), an abrupt rise of wall temperature due to a slight change in one of the flow variables. The temperature rise may be of two or three orders of magnitude, which most likely will cause a failure of the heated surface. Finding the CHF in terms of saturated evaporation is not straightforward. There is a wide variety of correlations that try to predict this condition and the corresponding location of the point of dry-out inside pipes, but there is not a correlation that provides satisfactory results under different geometries and working conditions of the fluid. So far, the Look-up tables method seems to be one that can give similar results to the experiments. Moreover, this method allows the extension of this application to different situations in a manner not too complicated. The implementation of this method in the code was made using the look-up tables of 2006 [4]. These tables are a function of pressure, mass flow and quality of steam. It is necessary to make a process of linear interpolation between the various tables that exist to find the CHF corresponding to the working conditions of the fluid.

The two-phase flow code has been validated with:

- Experimental data for low energy flow [5, 6, 7].
- Experimental data obtained at the CTTC laboratory using a vapor compression refrigeration system [8].
- Experimental data for high energy flow and correlations to predict the status of CHF [4, 9].

2.3. Radiation heat transfer modeling

Radiation heat transfer is studied at two different scales: on a large scale, consisting of an heliostat field and the tower, and on a small scale, comprising a section of the solar receiver tubes. Two different numerical models have been used to take into account the transport of heat due to radiation.

For the large scale case, in order to estimate the amount of energy that the heliostat field collects on the receiver section of the tower, an MCRT tool is used [10]. This kind of tool follows accurately the path of the solar rays, so the multiple reflections of solar and thermal radiation that occur on the tubes and plates of the receivers of solar power plants are accounted for naturally. The downside of this method is that it is computationally expensive, because a high number of rays must be shot to reduce statistical errors. However, from a computational perspective, each ray is independent of the others, and thus this method can be efficiently parallelized either using multiple processors or dedicated graphical processing units.

For the small scale case, the radiosity method is used. In a general situation, this method requires the knowledge of the specular view factors [10] between all the objects considered in the simulation. The radiosity method is very fast when compared to the MCRT method, although the complication lies in the determination of the specular view factors. Fortunately, the specular view factors can be computed with Montecarlo ray tracing techniques. The calculation is expensive in computational terms, but the accuracy can be traded by speed, as done for example by Miyanaga and Nakano [11]. The specular view factors thus calculated have been successfully compared against the ones given by Kang et al [12].

2.3.1. Coupling radiation and convection

The coupling between radiation and heat conduction has been considered in this stage. Any complicated physics inside the tubes (namely the two-phase flow) are ignored, and only heat conduction is solved on the tubes of the receiver. The tubes, on the other hand, radiate and receive heat according to their temperature and surface properties,

as well as the temperature and surface properties of the neighbor tubes. The solution to the heat conduction equation inside each tube gives its temperature, which determines the amount of radiated heat. With the temperature known, the radiosity method calculates the net radiative heat flux Q_r on each surface. An iterative process is required to converge to a solution. The natural convection of the air between the tubes is not solved at this stage. Its effect is added via a heat transfer coefficient that comes from the simulation of a simplified receiver geometry (section 3.3). Specifically, for the part of the tubes that receive solar radiation, the boundary condition is

$$-\lambda \frac{\partial T}{\partial n} = \alpha(T - T_g) + Q_r \quad (5)$$

2.4. The convection outside the tubes

The temperature differences between the tubes and the air surrounding them produce heat transfer by convection. This heat transfer is complicated to evaluate numerically (the geometry is complex and there are large differences between the diameter of the tubes and their length, the air conditions in the real case are variable in time and space, the temperature differences between the tubes and the air are high, etc.).

TermoFluids considers the resolution of the three-dimensional Navier-Stokes equations by means of Large Eddy Simulation (LES) or Direct Numerical Simulation. Different models can be used for modeling subgrid-scale tensor, e.g. the Wall-Adapting Local Eddy-viscosity model (WALE [13]).

The governing equations used in TermoFluids have been discretized on a collocated unstructured grid arrangement by means of second-order spectra-consistent schemes. Such schemes are conservative, i.e. they preserve the kinetic energy equation. These conservation properties are held if, and only if the discrete convective operator is skew-symmetric, the negative conjugate transpose of the discrete gradient operator is exactly equal to the divergence operator and the diffusive operator, is symmetric and positive-definite. These properties ensure both, stability and conservation of the kinetic-energy balance even at high Reynolds numbers and with coarse grids [14]. For the temporal discretization, in TermoFluids different numerical schemes are considered, e.g. Runge-Kutta scheme [15].

From the CFD&HT (computational fluid dynamics and heat transfer) numerical simulations, local and average Nusselt number are obtained. These parameters are then used for evaluating the heat transfer coefficients required by the heat conduction model.

3. Illustrative results

3.1. Heat conduction

In Fig. 2, an example of the distribution of dimensionless temperature is shown. This configuration corresponds with an array of tubes of a solar receiver with a similar design to the one depicted in Fig. 1b. Due to the incoming solar radiation, the temperature at the front side of the tubes is higher than that at the back side. As the fins between the tubes are not in direct contact with the circulating fluid inside the tubes they achieve high temperatures.

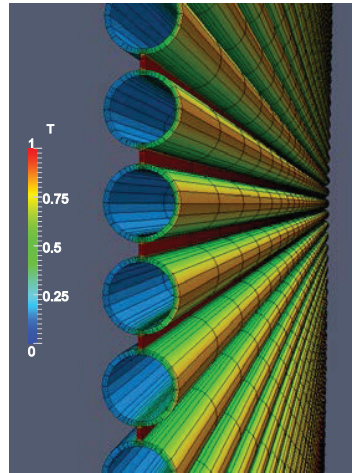


Fig. 2 Dimensionless distribution of temperature on a receiver formed by tubes with fins between them.

3.2. Radiation

The geometry considered in this situation consists of an arrangement of tubes and the receiver reflecting wall, as depicted in Fig. 3. The complete domain is this cross section extruded 10 times the diameter of the tubes. In this stage of the simulation, the tubes are completely solid, and therefore there is no phase-change phenomenon occurring inside the tubes. There is also no heat conduction between the tubes and the receiver wall.

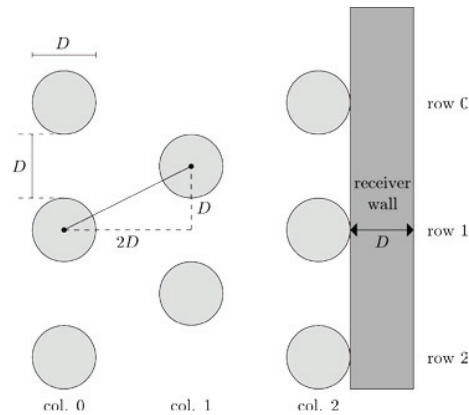


Fig. 3 Geometry of the receiver section. Radiative properties of tubes are different for each half of the tube.

The radiative properties of the tubes have been separated in the solar and thermal bands, to allow for more flexibility when defining the case. The radiosity equation is then solved twice, one time per each band. In particular, the emissivity for the solar and thermal bands is 0.93 and 0.1 respectively. Only specular reflectivity is taken into account. The receiver wall has a high reflectivity for the solar radiation to have a second chance to be absorbed by the tubes. To simulate the radiation coming from the heliostat field, a source term is calculated at different incidence angles with respect to the normal of the receiver wall. This source term is added only for the solar band. For the thermophysical properties, those of copper have been used for all the materials.

The tubes have one inlet boundary at a fixed temperature, while the temperature at all other boundaries is calculated taking into account the convective and radiative heat fluxes due to the environment and the other tubes. The temperature T_g in equation 5 depends on the column of the tube. Specifically, the temperatures are 425K, 575K, and 675K for the columns 0, 1, and 2 respectively. These temperatures are taken from a previous numerical simulation of the natural convection between the tubes. The heat transfer coefficient is calculated from the Nusselt number as explained in section 2.1. The receiver wall shares this same boundary condition, except for the wall opposed to the tubes where the temperature has been fixed.

In Fig. 4 the temperature of the tubes and the plate is shown for different angles of incidence of the solar radiation to the receiver. In the case of normal incidence (Fig. 4a), the radiation is absorbed by the first two columns of tubes (column 0 and column 1). In the case of incidence at an angle of 45 degrees (Fig. 4b), the temperature distribution is less uniform. The tubes in column 2 reach the highest temperatures, because the T_g is maximal in this situation (and these tubes loss heat due to convection to an ambient at a much higher temperature), and furthermore this column also receives a sizable amount of incoming solar radiation.

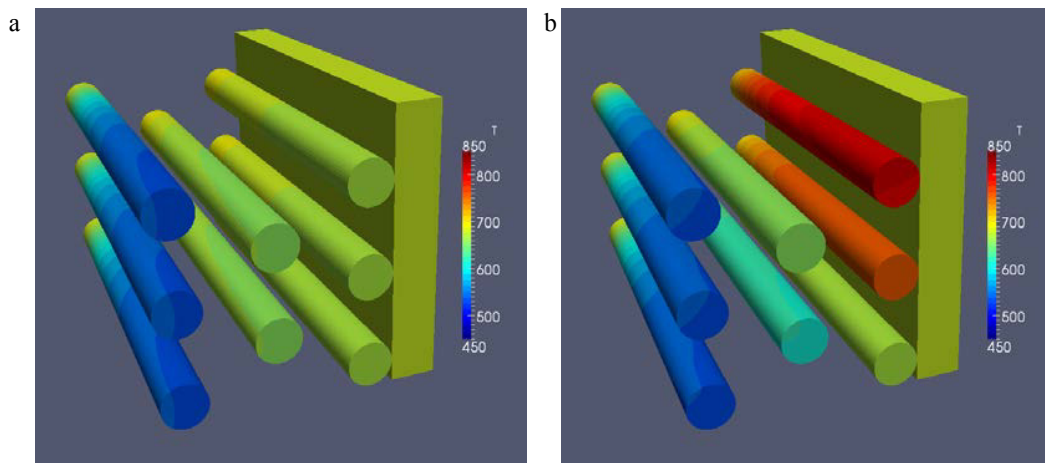


Fig. 4 Temperature of the section of the receiver. Solar radiation incides at different angles. (a) Incidence angle is zero; (b) incidence angle is 45 degrees.

3.3. Convection

In order to reduce the complexity of the problem some assumptions have been made:

- The tubes have been considered isothermal.
- Only natural convection occurs (no wind) and the temperature of the air away from the tubes is constant.
- The air has been supposed an incompressible Newtonian fluid, with constant thermophysical properties and negligible interaction in radiation.

Under these assumptions, numerical simulations of natural convection in a section of a receiver with three rows of vertical tubes have been carried out by means of LES using the WALE model for modeling the subgrid-scale tensor.

3.3.1. Problem definition an numerical domain

The situation under consideration in the simulations has been natural convection of air ($Pr = \nu/\alpha = 0.71$) in a section of a solar receiver with three rows of vertical tubes (see Fig. 5a) with a Rayleigh number, based on the

height of the tubes $Z = 6D$, of $Ra = g\beta(T_h - T_c)((Z1)^3 Pr)/\nu^2 = 10^8$. The length and width of the domain are $X = 6.5D$ and $Y = 2D$ respectively.

The vertical red tubes are considered to be isothermal with temperature $T_h = 893.15 K$. The yellow section is considered as an adiabatic wall. No slip conditions are set at the solid walls. The flow has been considered periodic in the z axis and in the y axis. Pressure boundary condition is imposed at the open boundary in the x axis, with Neumann condition for temperature if the air goes out of the domain and temperature $T_c = 293.15 K$ if it goes in.

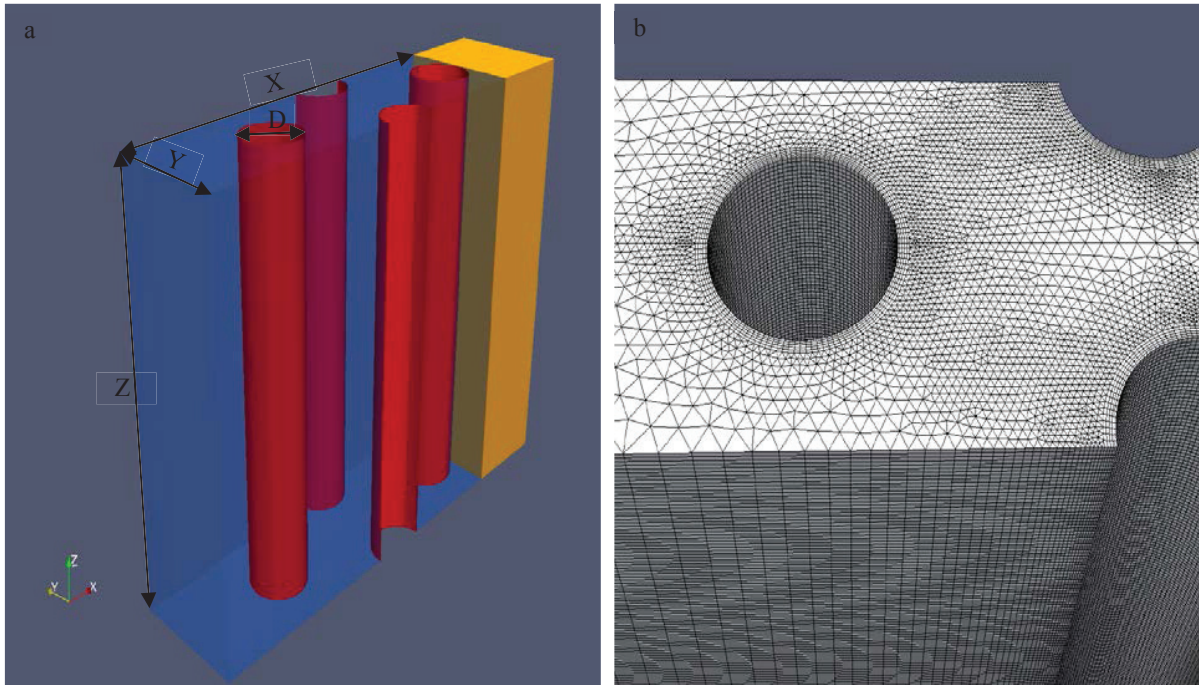


Fig. 5. (a) Scheme of the section of the solar receiver; (b) mesh detail.

The meshes used for solving the domain considered have been generated by a constant step extrusion in the z axis of a two-dimensional (2D) unstructured grid (see Fig. 5b for a close view of the mesh). Under these conditions, the span-wise coupling of the discrete Poisson equation, which results from the incompressibility constraint, yields circulant sub-matrices that are diagonalizable in a Fourier space. This allows to solve the Poisson equation by means of a Fast Fourier Transform method. The algorithm used is based on the explicit calculation and direct solution of a Schur Complement system for the independent 2D systems. For more details the reader is referred to [15].

The number of control volumes of the final mesh has been 11,904 by 256 planes (about 3 million control volumes). In order to properly evaluate the heat flux at the surface of the tubes, a prismatic layer has been used for the control volumes close to the tubes.

3.3.2. Results

The simulation has been started with the air temperature set to T_c . Then, the simulation has been advanced in time until statistical stationary flow conditions have been achieved. After the initial transient has been completely washed out, averaged statistics have been computed. The averaged statistics presented in this paper have been obtained by averaging the computed variables in time and homogeneous direction.

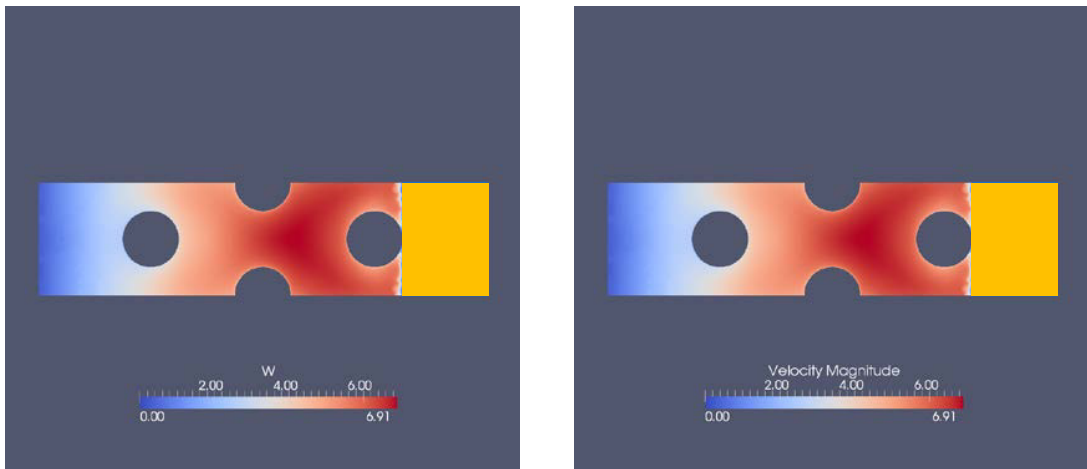


Fig. 6. (a) Component in the z axis of the average flow velocity; (b) magnitude of the average flow velocity.

In Fig. 6 the distribution of the component in the z axis of the velocity and the averaged magnitude of the velocity are shown. It can be observed that the average flow is strongly driven upwards along the tubes.

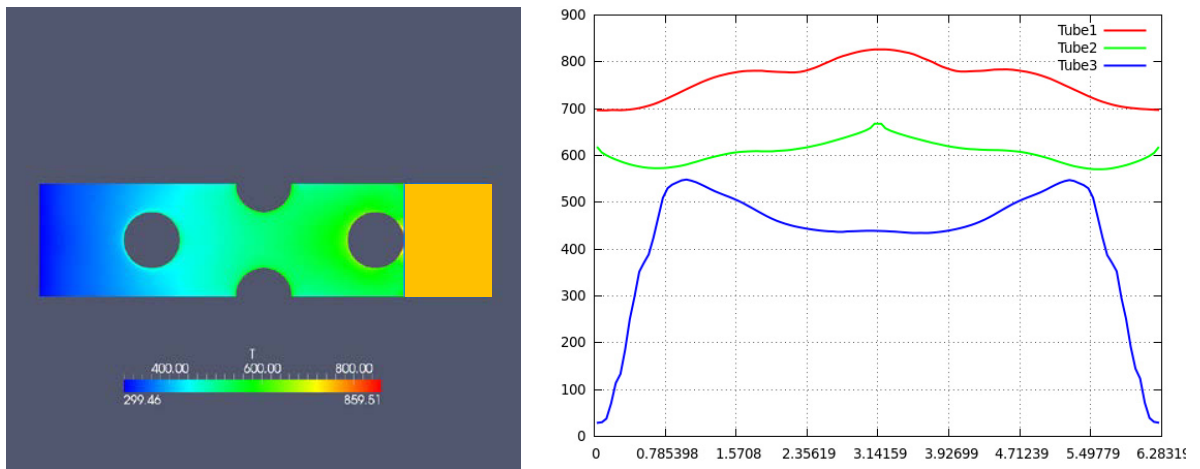


Fig. 7. (a) Average air temperature; (b) average Nusselt number around the tubes.

In Fig. 7 the average Nusselt number around the tubes is presented. Tube1 is the closest one to the open boundary and Tube3 is the one next to the adiabatic wall. The value of the Nusselt number decreases when the tubes are closer to the center of the receiver due to the increase of the temperature of the air.

4. Conclusions

The methodology to simulate heat transfer and fluid dynamics phenomena in the receiver of a solar tower has been presented. In section 2, models for the heat conduction in solids, two-phase flow, solar and thermal radiation and natural convection have been described and thoroughly validated against different experimental and numerical results. The results of the numerical simulation of the tubes of the solar tower receivers have been presented in section 3.

In the current state, a highly detailed CFD simulation of the natural convection around the tubes provides the data to the simplified models: the simulation of the two phase fluid in the tubes uses the estimated convective heat transfer coefficient, and the simulation of radiation heat losses uses the average temperature in the vicinity of the tubes. This paper shows the ability of performing these complex simulations with present day technology.

The methodology presented above is currently being used for the CFD&HT modeling of a full-scale solar tower receiver. At the time this contribution is written, only a few instants of the complex unsteady fluid-dynamic and heat transfer phenomena have been simulated.

Acknowledgements

This work has been financially supported by the Ministerio de Educación y Ciencia, Secretaría de Estado de Universidades e Investigación, Spain (ref. ENE2010-17801) and by the Collaboration Project between Universidad Politècnica de Catalunya and Termo Fluids S.L.

References

- [1] NREL, National Renewable Energy Laboratory. Concentrating Solar Power Projects, <http://www.nrel.gov/esp/solarpaces/>
- [2] Lehmkuhl O., Pérez Segarra C. D., Borrell R., Soria M. and Oliva A., 2007. TermoFluids: A new Parallel unstructured CFD code for the simulation of turbulent industrial problems on low cost PC Cluster. Proceedings of the Parallel CFD 2007 Conference, pg. 1–8.
- [3] Morales Ruiz S., Rigola J., Pérez Segarra C.D. and García Valladares O., 2008. Numerical analysis of two-phase flow in condensers and evaporators with special emphasis on single phase-two phase transition zones. Applied Thermal Engineering 29, pg. 1032–1042.
- [4] Groeneveld D.C., Shan J.Q., Vasic A.Z., Leung L.K.H., Durmayaz A., Yang J., Cheng S.C. and Tanase A., 2007. The 2006 CHF Look-up table, Nuclear Engineering and Design, vol 237, pg. 1909–1922.
- [5] Kattan N., Thome J.R. and Fravrat D., February 1998. Flow Boiling in Horizontal Tubes: Part I - Development of a Diabatic Two-Phase Flow Pattern map, Journal of Heat Transfer, vol. 120, pg. 140–147.
- [6] Cavallini A., Censi G., Del Col D., Doretti L., Longo G.A. and Rossetto L., 2001. Experimental Investigation on Condensation Heat Transfer and Pressure Drop of New HFC Refrigerants (R134a, R125, R32, R410A R236ea) in a Horizontal Smooth Tube, Int. Journal of Refrigeration, vol. 24, pg. 73–87.
- [7] Jung D.S. and Didion A., 1989. Electrical Power Research Institute (EPRI) ER- 6364, Research Project 8006-2.
- [8] Rigola J., Pérez Segarra C.D., and Oliva A., 2003. Modelling and numerical simulation of the thermal and fluid dynamic behaviour of hermetic reciprocating compressors - part 2: Experimental investigation. Int. Journal of Heating Ventilating Air Conditioning and Refrigeration Research, 9(2), pg. 237– 250.
- [9] Wong Y.L., Groeneveld D.C. and Cheng S.C., 1990. CHF prediction for horizontal tubes. Int. Journal of Multiphase Flow, 16, pg. 123–138.
- [10] Michael F. Modest. Radiative Heat Transfer. McGraw Hill, 1993.
- [11] Toshiyuki Miyayama and Yukio Nakano. Radiation heat transfer in three dimensional closed space including diffuse and specular surfaces. Heat Transfer - Asian Research, vol 32(2) 2003, p. 108–129.
- [12] Sae Byul Kang, Woo Il Lee, Joon Sik Lee. An effective calculation method for radiative exchange in an enclosure with specular surfaces. Numerical Heat Transfer, Part A, vol 50, 2006, p. 865–881.
- [13] Nicoud F. and F. Ducros, 1999. *Subgrid-scale stress modelling based on the square of the velocity gradient tensor*. Flow, Turbulence and Combustion, 62:183–200.
- [14] Verstappen R.W.C.P. and Van Der Velde R.M., Symmetry-Preserving Discretization of Heat Transfer in a Complex Turbulent Flow, Journal of Engineering Mathematics 54 (4) (2006) 299–318.
- [15] Borrell R., Lehmkuhl O., Trias F. and Oliva A.. Parallel direct Poisson solver for discretisations with one Fourier diagonalisable direction, Computational Physics, Vol. 230, No. 12, 2011, pp. 4723–4741.